Using RotCFD to Predict Isolated XV-15 Rotor Performance

Witold J. F. Koning[1] and C. W. Acree, Jr.[2]
NASA Ames Research Center, Moffett Field, California, 94035

Ganesh Rajagopalan[3]
Iowa State University, Ames, Iowa, 50011

The objective of the present research is to validate an isolated XV-15 rotor computational model. The predicted performance of the XV-15 rotor during various flight modes is compared to wind-tunnel data. For computational efficiency, a simple rotor model is coupled to a full CFD flow-field analysis. A hybrid RANS solver, RotCFD, is used with an unsteady, incompressible flow model and a realizable k-ε turbulence model. The rotor is modeled using an actuator disk with a momentum source approach. RotCFD is a useful engineering tool because the problem setup, grid generation, and solver execution is faster than many CFD codes. With a stall-delay model, RotCFD predictions match OARF hover data quite well; RotCFD also matches wind-tunnel data for tilt rotor mode. RotCFD matches airplane-mode wind-tunnel data better at low speed than at high speed. However, the tip-loss model used proved to be too aggressive. Future work will investigate wind-tunnel wall effects on isolated rotor performance with the eventual goal of modeling a complete wind tunnel installation.

Nomenclature

BEMT	=	blade-element momentum theory
c	=	blade chord
c_l	=	section lift coefficient
$c_{l,\text{table}}$	=	section lift coefficient from airfoil table
C_P	=	power coefficient
C_T	=	thrust coefficient
K_L	=	stall-delay lift parameter
M_{tip}	=	tip Mach number
N	=	number of blades
r	=	blade or rotor disk radial coordinate
R	=	rotor radius
V	=	rotor or rotorcraft velocity
x, y, z	=	CFD grid coordinates
α_p	=	pylon tilt angle
Ω	=	rotor rotational speed
μ	=	advance ratio $V/\Omega R$
σ	=	rotor solidity
CAMRAD	=	Comprehensive Analytical Model of Rotorcraft Aerodynamics and Dynamics
CFD	=	Computational Fluid Dynamics
k-ε	=	(realizable) k-ε two-equation turbulence model [1], [2]
NFAC	=	National Full-Scale Aerodynamics Complex
OARF	=	Outdoor Aerodynamic Research Facility
RANS	=	Reynolds Averaged Navier-Stokes
RotCFD	=	Rotorcraft CFD
RotUNS	=	Rotorcraft Unstructured Solver
SD	=	stall delay
TL	=	tip loss
URANS	=	Unsteady Reynolds Averaged Navier-Stokes

[1] Graduate Student, Aerospace Engineering, Delft University of Technology.
[2] Aerospace Engineer, Aeromechanics Office, NASA Ames Research Center.
[3] Professor, Aerospace Engineering, Iowa State University.

Presented at the AHS Technical Meeting on Aeromechanics Design for Vertical Lift, San Francisco, CA, January 20-22, 2016.

I. Introduction

Experimental techniques to measure rotor and airframe aerodynamic performance are widely used but the need exists to understand the limitations of ground based testing by augmenting the analysis of experimental test results with Computational Fluid Dynamics (CFD) modeling. The long-term objective of the present research is to develop an XV-15 Tilt Rotor Research Aircraft rotor model for investigation of wind tunnel wall interference. Ultimately the rotor model developed will be used to investigate wind tunnel wall effects on large tilt rotors in the National Full-Scale Aerodynamics Complex (NFAC) facility. The interest in civil tilt rotors originates from NASA studies indicating significant reduction in congestion of commercial transport aviation [3].

The focus of this research is to understand the limitations and accuracy of tilt rotor performance predictions using a hybrid CFD program. Rotorcraft CFD (RotCFD) is a mid-fidelity CFD tool specifically for rotorcraft design efforts and has been developed recently [4], [5]. RotCFD uses a RANS solver to simulate unsteady, incompressible flow with a k-ε turbulence model. Options for modeling the rotor include an actuator disk model or blade element model. Both options use two-dimensional airfoil data, which allows for relatively fast simulations of unsteady rotorcraft cases. The rotor is represented solely through the momentum it imparts to the flow. The rotor is coupled with the surrounding flow by representing the rotor as sources in the momentum equations. This representation differs from the classical way of resolving a very fine grid around the rotor geometry to capture all flow effects, giving RotCFD a significant advantage in simulation time.

Using two-dimensional airfoil data and a traditional blade element model or actuator disk model omits all three-dimensional effects. Most notable effects are stall delay, tip loss, yawed flow effects and unsteady rotor aerodynamics. Care must be taken that these effects are properly accounted for either within RotCFD or by applying corrections to the airfoil data tables in C81 format.

To validate RotCFD, the XV-15 rotor is used as a reference large-scale proprotor. As long as rotor area, solidity, and tip speed are generally similar, any two proprotors will experience the same interference effects. The XV-15 has an extensive experimental database, which makes it uniquely useful for validation. This paper documents the first, critical step in validation, which is to demonstrate that RotCFD can predict isolated rotor performance.

CAMRAD II (Comprehensive Analytical Model of Rotorcraft Aerodynamics and Dynamics) is a useful tool for examining the effects of different modeling assumptions on proprotor performance. CAMRAD II uses exactly the same airfoil tables as RotCFD and offers multiple stall-delay and tip-loss models [6]. CAMRAD II can be run using only blade-element momentum theory, or with any of several variations on prescribed- and free-wake models. Although CAMRAD II executes much faster than RotCFD, the wake model is not suitable for computing wind-tunnel wall effects. CAMRAD II's fast execution speed was here exploited to generate XV-15 performance trends to illustrate the relative importance of stall-delay and tip-relief effects to help validate RotCFD. While CAMRAD's wake models can provide very good correlation with test data, they have to be matched to the particular rotor and flight conditions being analyzed. Setting up the appropriate wake model typically requires considerable judgment and often much effort for good results.

II. Tilt Rotor Characteristics

Tilt rotors have the capability to hover, fly in airplane mode, or fly in tilt rotor mode. Each of these modes has their own characteristics and needs to be properly evaluated. Hover is the defining characteristic of a helicopter; during hover the rotor produces lift but has no relative velocity to the air. A time-accurate representation of the wake and performance is very complicated to accurately compute. The analysis of a free field hover case also poses as the most computationally expensive as the rotor wake and inflow are solely developed by the rotor: no free stream component is present and thus relatively slow convergence occurs. Furthermore, the boundaries must be set relatively far from the rotor in order to not influence the flow field.

During edgewise forward flight the rotor moves though the air with a small forward tilt. This forward tilt creates the small forward component of the thrust vector that provides the propulsive force for the helicopter. Different flow phenomena arise here, in contrast to hover. Because of the freestream flow of air, the advancing side of the rotor will experience a higher relative velocity than the retreating side of the rotor. This asymmetry of lift is normally accounted for by rotor flapping. For the RotCFD analysis reported here, rotor trim is not considered and the total trust produced during trimmed forward flight is assumed comparable to the untrimmed averaged rotor.

If the tilt rotor's pylon is lowered to airplane mode the rotor acts like an airplane propeller. Pylon angles between airplane and hover mode will be called tilt mode and exhibit characteristics of both modes. Flight modes are considered with only thrust values well within the XV-15's flight envelope. Furthermore, neither steady nor unsteady aeroelastic effects will be considered.

III. Description of RotCFD

Computational Fluid Dynamics (CFD) is often seen as one of three most important parts of modern aerodynamics, together with pure experiment and pure theory. Accurate computation of the flow field around a helicopter is a highly complicated task in aerodynamics. While the Navier-Stokes equations can theoretically be solved to yield a high accuracy solution, several assumptions regarding the complexity of the flow are needed to make efficient computation feasible within the given timeframe and computational budget.

RotCFD [5] uses an Integrated Design Environment (IDE) specific to rotorcraft but also capable of simulating a wide range of aerodynamic problems. The IDE emphasizes user friendliness and efficiency to streamline the analytical process from geometry to CFD solution. The key components of RotCFD are a geometry module, a semi-automated grid generation module, a flow-solver module, a rotor module, and a flow-visualization module, all integrated into one user environment.

The flow solver needs to handle unsteady rotor simulations while being computationally inexpensive. Rotorcraft Unstructured Solver (RotUNS) is a module within RotCFD that uses three-dimensional, unsteady, incompressible Reynolds-Averaged Navier-Stokes equations (URANS) on a hybrid unstructured topology. RotCFD uses a Cartesian unstructured off-body grid and a tetrahedral unstructured on-body grid. However, for the XV-15 model used here, the blade sections are not gridded. Spalart discusses the possible pitfalls with the use of URANS but also indicates that URANS is one of the few feasible unsteady methods when computational budget is limited [7].

Turbulence is accounted for by the RANS equations combined with a two-equation realizable k-ε turbulence model with special wall treatment. Jones and Launder [1], [2] presented and validated the k-ε turbulence model in the 1970s. Yu & Cao [8] have shown that accurate CFD analyses for the flow field and performance of a helicopter in forward flight can be obtained with a k-ε turbulence model with wall function method.

Discretization is done using the finite-volume method and an implicit solver has been used in order to have a less stringent stability criterion and therefore more flexibility for various operations.

RotCFD offers two different rotor solutions, an actuator-disk model and a discrete-blade model. Both methods rely on external tables of two-dimensional airfoil coefficients. Blade element momentum theory, including swirl terms, is used to compute each blade section's lift, drag and pitching moment from the airfoil tables. The section forces and moments are then converted to source terms which are added to the momentum equations at the grid points where the rotor blades intersect. The actuator-disk solution implicitly couples the external flow field to the rotor via integrated momentum sources, whereas the discrete-blade solution couples the external flow to individual lifting lines, one for each blade. The discrete-blade method is more computationally demanding than the actuator-disk method. Both models provide a less computationally intensive method compared to true viscous unsteady blade modeling. This greatly simplifies the simulation by omitting the computation of a time-accurate boundary layer interacting with the unsteady rotor geometry and outside flow on a very dense grid. Therefore both models reduce computation time while still yielding a reasonably accurate representation of the rotor aerodynamics [9]. For example, performance converged for the XV-15 isolated rotor in hover on a 2.5-GHz Intel i5 processor with 4 threads in less than half a day with an implicit solver, steady model, around 10^6 cells, and 10^3 time steps.

This hybrid approach, a simplified rotor model with a computed (not modeled) wake, is ideal for assessing aerodynamic interaction problems. Computation proceeds much faster than full CFD (which explicitly includes the geometry of each rotor blade) and provides more detailed flow-field calculations, including explicit wind-tunnel wall effects, than any wake model.

The present paper provides RotCFD results for the actuator-disk solution only. This approach is sufficient to validate the method against experimental data, which is the immediate purpose of the research. The method is also sufficient to capture wind-tunnel interference effects, which is the longer-term motivation.

Table 1. RotCFD simulation parameters for the XV-15 rotor

	Hover	**Tilt Mode**	**Airplane**
tip speed, m/s	225.55	221.17	183.76
number of time steps	1000	500	500
step size (deg azimuth)	8.5	8.3	6.9
number of rotor revolutions	23.6	11.5	9.6
total number of grid cells	1,053,948	2,029,692	2,029,692
computational domain (relative to rotor center):			
$\pm x/R$	± 10	± 10	± 10
$\pm y/R$	± 10	± 10	± 10
$\pm z/R$	+10, -18	+10, -18	+10, -18
wall boundary conditions:			
min x/R	pressure	$Vx=Vy=0;Vz=-V_\infty$	$Vx=Vy=0;Vz=-V_\infty$
max x/R	pressure	$Vx=Vy=0;Vz=-V_\infty$	$Vx=Vy=0;Vz=-V_\infty$
min y/R	pressure	$Vx=Vy=0;Vz=-V_\infty$	$Vx=Vy=0;Vz=-V_\infty$
max y/R	pressure	$Vx=Vy=0;Vz=-V_\infty$	$Vx=Vy=0;Vz=-V_\infty$
min z/R	mass outflow	mass outflow	mass outflow
max z/R	pressure	$Vx=Vy=0;Vz=-V_\infty$	$Vx=Vy=0;Vz=-V_\infty$

Table 1 provides the RotCFD temporal settings, total grid sizes, domain dimensions, and wall boundary conditions for the hover, tilt-, and airplane-mode calculations. Figure 1a shows an oblique view of the computational domain, which was the same for all cases. A cross-section of the grid used for the hover cases is shown for the plane x=0. A top view of the domain is shown in Figure 1b for z=0. The x-y-z coordinate system is located at the rotor center. A refinement box was added to provide a denser grid to capture the rotor wake in hover. For the tilt- and airplane-mode cases, the freestream velocity was in the negative z-direction (from top to bottom in Figure 1). The refinement box for the transition and airplane modes cases was extended to the bottom (minimum z) of the domain and also adjusted in width to better capture the wake in edgewise and axial flight.

IV. Airfoil Data Corrections

RotCFD depends on two-dimensional airfoil tables, so stall delay and tip loss must be explicitly accounted for. The approach used here was to modify the airfoil tables to include stall delay and tip loss corrections, as explained below. Because the XV-15 airfoil data tables were acquired for full-scale airfoils, no scaling corrections, including Reynolds number effects, were needed.

Similar to aircraft wings, trailed vortex inflow over the tip of a rotor blade reduces the blade's lifting capability. RotCFD, however, uses two-dimensional airfoil data and thus experiences section lift up to the blade tip. Leishman [10] describes the effective blade radius—usually around 98% of the blade radius—that is unaffected by tip loss. The lift at the remaining 2% of the blade drops to zero at the tip. This approximation is chosen here for its simplicity.

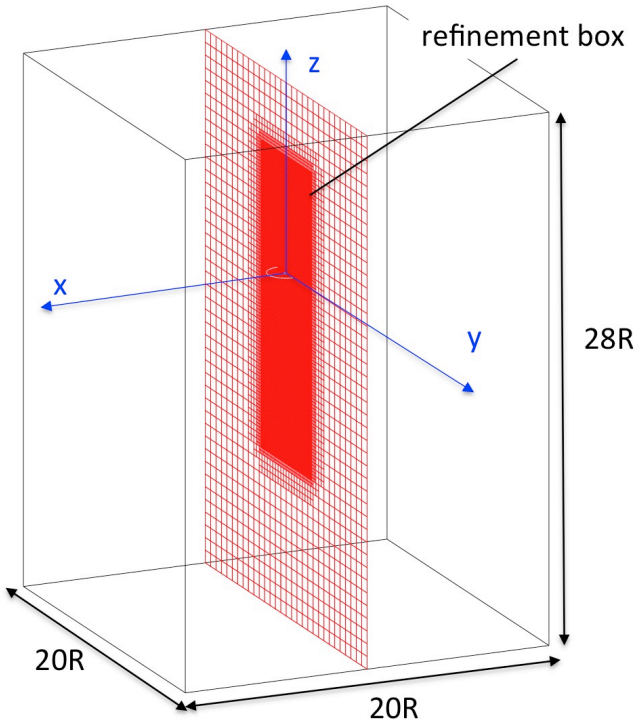

a)

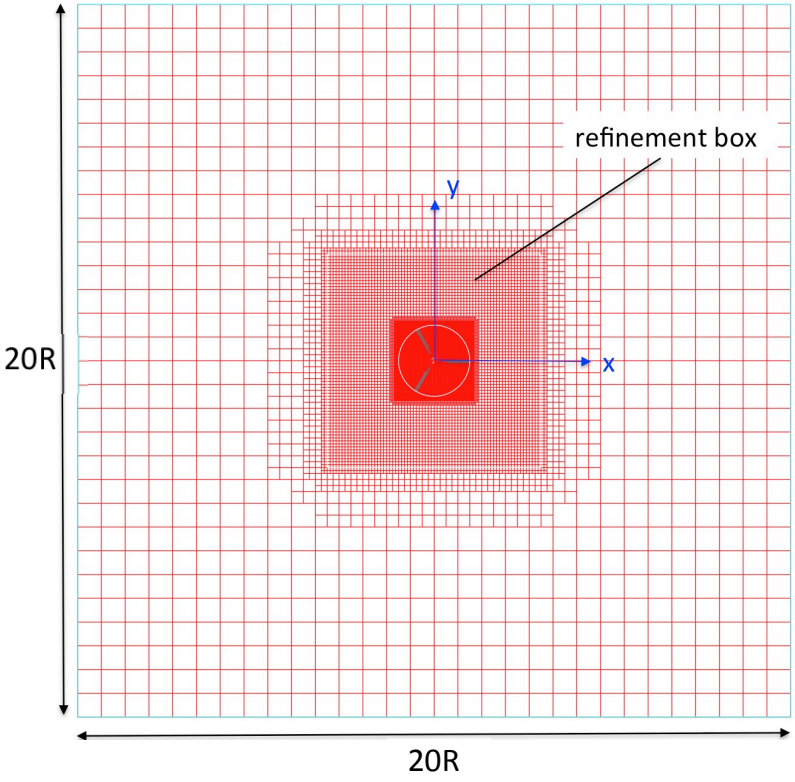

b)

Figure 1. RotCFD computational domain and grid system for hover cases: a) oblique view of x=0 plane; b) top view of z=0 plane.

Modeling the effect of a rotor's rotation on the boundary layer is crucial for correctly predicting rotor performance [11], primarily during hover. Since RotCFD uses 2D airfoil tables, the boundary layer will not be resolved during the simulations. One approach for accommodating the boundary layer rotational effect is altering the airfoil data tables. Acree describes modeling requirements for analysis and optimization of the JVX proprotor performance [12], which is more technically advanced than the XV-15 rotor but has similar aerodynamic behavior, notably significant stall delay in hover. An approach to modeling stall delay is described in Corrigan [11]. The Corrigan stall delay model uses augmentation of the lift values in the airfoil data tables by multiplying the section lift coefficient with a stall delay factor, K_L, as shown in Equation (1).

$$K_L = \left(\frac{c/r}{0.136}\left(\frac{0.1517}{c/r}\right)^{1/1.084}\right)^{1.8} = (1.291(c/r)^{0.0775})^{1.8} \quad (1)$$

The section lift is subsequently computed using Equation (2):

$$c_l = K_L c_{l,table}(\alpha/K_L) \quad (2)$$

The XV-15 airfoils vary linearly with radius, but the stall delay is non-linear. Because the stall delay is spanwise non-linear, the computational radial stations must be interpolated, even if the spanwise lift distribution is fairly linear. A MATLAB code was written to perform a triple interpolation over angle of attack, Mach number and radial station. Once the angle of attack and Mach number distributions (interpolated) are uniform over the radial stations, the Corrigan stall delay model is applied over a user-defined set of blade stations (Figure 2).

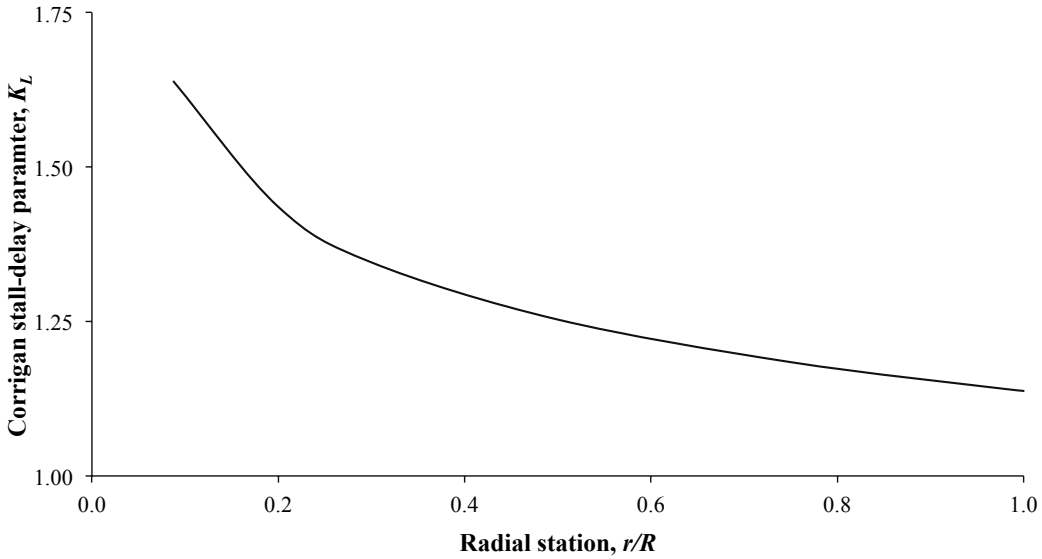

Figure 2. Spanwise Corrigan stall delay parameter obtained for the XV-15 rotor model.

Although the largest effect of stall delay is seen near the root (Figure 2), the tip also shows significant stall delay using this model. The stall delay is applied from 0 deg up to 30 deg angle of attack. From 30 deg to 60 deg the model is linearly washed out. The stall delay is only applied for positive section lift which is assumed to occur for an angle of attack greater than 0 deg. The zero lift angle of attack was close to, but not exactly equal to, zero and therefore small errors in the stall delay model might be introduced. These errors are assumed to be negligible as the section lift within the angle of attack range from zero to zero-lift is very small.

IV. Validation Process

The XV-15 rotor (and aerodynamic data tables and airfoils) was used for this research because the existing test data (wind tunnel and flight) are publically available. Also, the XV-15 flight test data reports provide background in understanding the XV-15 and its performance [13]. The experimental data presented here are taken from isolated rotor tests, discussed below.

The geometric blade solidity was used with the RotCFD calculations since only aerodynamic sections of the blade were modeled in this analysis (no hub or non-aerodynamic blade parts were included), as shown in Equation (3). A solidity value of 0.089 is reported in [14] and was used for the CAMRAD II predictions. The value of solidity most commonly reported for the XV-15 (σ=0.089) appears to assume that the chord extends all the way to zero radius. The actual blade has both root taper and root cutout; the majority of the blade has constant chord.

$$\sigma = \frac{NcR_e}{A} = \frac{NcR_e}{\pi R^2} \approx 0.081 \qquad (3)$$

where R_e is the equivalent radius to get the literal geometric value of solidity. For the RotCFD analyses reported here, the blade chord is assumed constant at the value at $0.75R$, hence the RotCFD results are scaled to σ=0.081.

The XV-15 hover data set was acquired on the Prop Test Rig (Figure 3) at the Outdoor Aerodynamic Research Facility (OARF) by Felker et al. [15]. The data are referred to as the "OARF Data" in this report. The OARF Data are the only full-scale data without wall effects for an XV-15 isolated rotor in hover. The Bell Helicopter company documented the performance of an XV-15 isolated rotor in the NFAC facility [16] under various conditions (Figure 3). Johnson [17] performed an assessment of the capability to calculate tilt rotor aircraft performance based on data in that report. Johnson's paper relied upon an earlier and much less capable comprehensive analysis than CAMRAD II. For predicting isolated proprotor performance, the most significant updates are an improved free-wake model and the introduction of stall-delay models in CAMRAD II [6]. Here, the model developed by Corrigan and Schillings was used [11]. The CAMRAD II results reported here constitute an update to those reported in [17].

Figure 3. XV-15 rotor in the NFAC (left) and at the OARF (right).

The XV-15 rotor blade has 1-deg sweep that was not incorporated into the RotCFD model because the sweep exists only for structural reasons. The main parameters that are needed for the rotor are the twist and chord distribution, two-dimensional airfoil data along the span of the XV-15 blade, and the characteristic dimensions of the rotor. Some conflicting values were found in different publications [14]-[16], [18]-[19]. The XV-15 rotor has root taper that is not always explicitly included in the given value of solidity. Also, the XV-15 was flown with multiple hub configurations with different precone. The final values given here were decided in collaboration with experienced XV-15 researchers. The rotor parameters are summarized in Table 2. The value of the precone in Table 2 was that used for the OARF test data set [15].

Table 2. XV-15 Rotor Characteristics [14]-[16], [18]-[19].

Blade Geometry	
Diameter	25 ft
Disc area	491 ft^2
Constant-section blade chord	14 in
Blade area	43.75 ft^2
Root cutout	0.0875 r/R
Solidity	0.089
Blade Twist (bilinear)	
Chord-line aerodynamic	38.7 deg
Total chord twist	41.5 deg
Blade Airfoil Section	
0.0875 [r/R]	NACA 64-X25
0.2500 [r/R]	NACA 64-X25
0.5268 [r/R]	NACA 64-X18
0.8093 [r/R]	NACA 64-X12
1.0000 [r/R]	NACA 64-X08
Rotor Characteristics	
Hub precone angle	2.5 deg
Rotor speed	
Helicopter mode (hover, edgewise)	589 rpm
Airplane mode (axial)	517 rpm
Blade tip speed	
Helicopter mode (hover, edgewise)	740 ft/s
Airplane mode (axial)	600 ft/s

VI. Results

1. Hover

Figure 4 shows the RotCFD hover solution (no tip loss, no stall delay) for a collective pitch of 6 deg after nearly 19 rotor revolutions. Although Figure 4b shows that the starting vortex has not reached the bottom of the computation domain, the rotor forces have already reached a steady value.

Spatial and temporal resolution within RotCFD were checked for any effect on the result. Also, relaxation factors and number of iterations were varied to check for deviations. Finally, a non-rotating spinner body was placed in the XV-15 root cutout to check the influence of hub geometry on performance. None of the aforementioned changes showed significant effect on predicted rotor performance.

Figures 5 and 6 show XV-15 hover data at two tip Mach numbers. There are very minor differences in performance between the two Mach numbers.

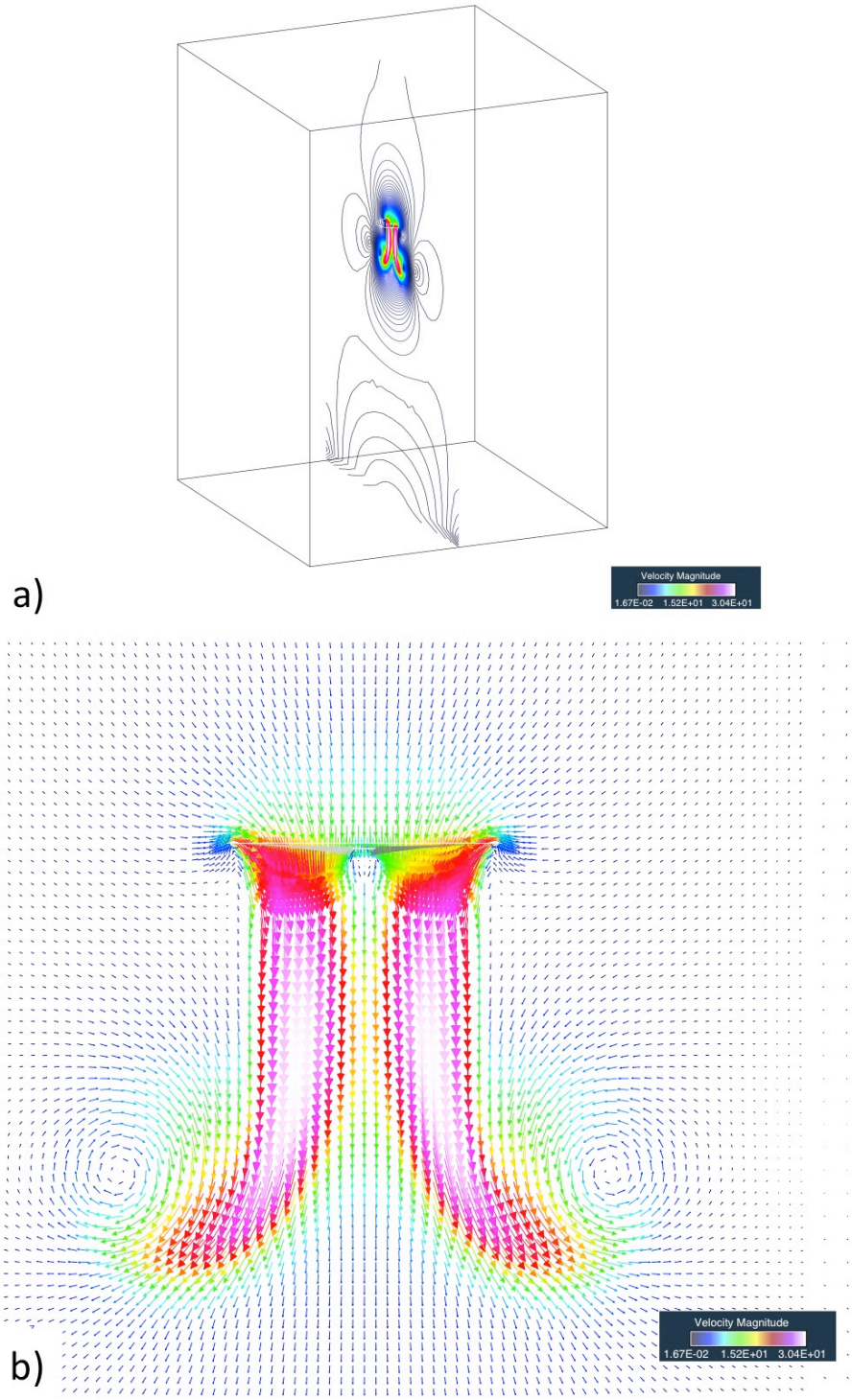

Figure 4. Hover solution, collective pitch = 6 deg, time=2 sec (18.8 revolutions):
a) velocity magnitude contours for x=0 plane; b) close-up of velocity vector field in the x=0 plane

All possible combinations of tip loss (TL), stall delay (SD), and unaltered configurations were evaluated with RotCFD for hover. RotCFD calculations of XV-15 hover performance are shown in Figure 5 for all four cases, always for M_{tip}=0.66. The results for the combined case ("RotCFD TL SD") lie almost on the same thrust-power curve as the unaltered, clean results. The tip-loss-only case ("RotCFD TL") predicts tip effect and the stall-delay-

only case ("RotCFD SD") shows reasonable agreement with the OARF and CAMRAD II data, although not as good as the combined case .

CAMRAD II predictions using a free-wake model and Corrigan stall delay ("Free wake SD") are also shown in Figure 5, along with predictions with no stall delay. Predictions with blade-element momentum theory (BEMT), here using the Prandtl tip-loss correction with stall delay, are also shown for reference ("BEMT TL SD"). The CAMRAD II free-wake predictions with the Corrigan stall-delay model (solid gray line) closely match the data, even in the post-stall region. The excellent results obtained with CAMRAD benefited from many years of developmental effort, whereas the RotCFD results were obtained within a few weeks, including constructing the XV-15 rotor model from scratch.

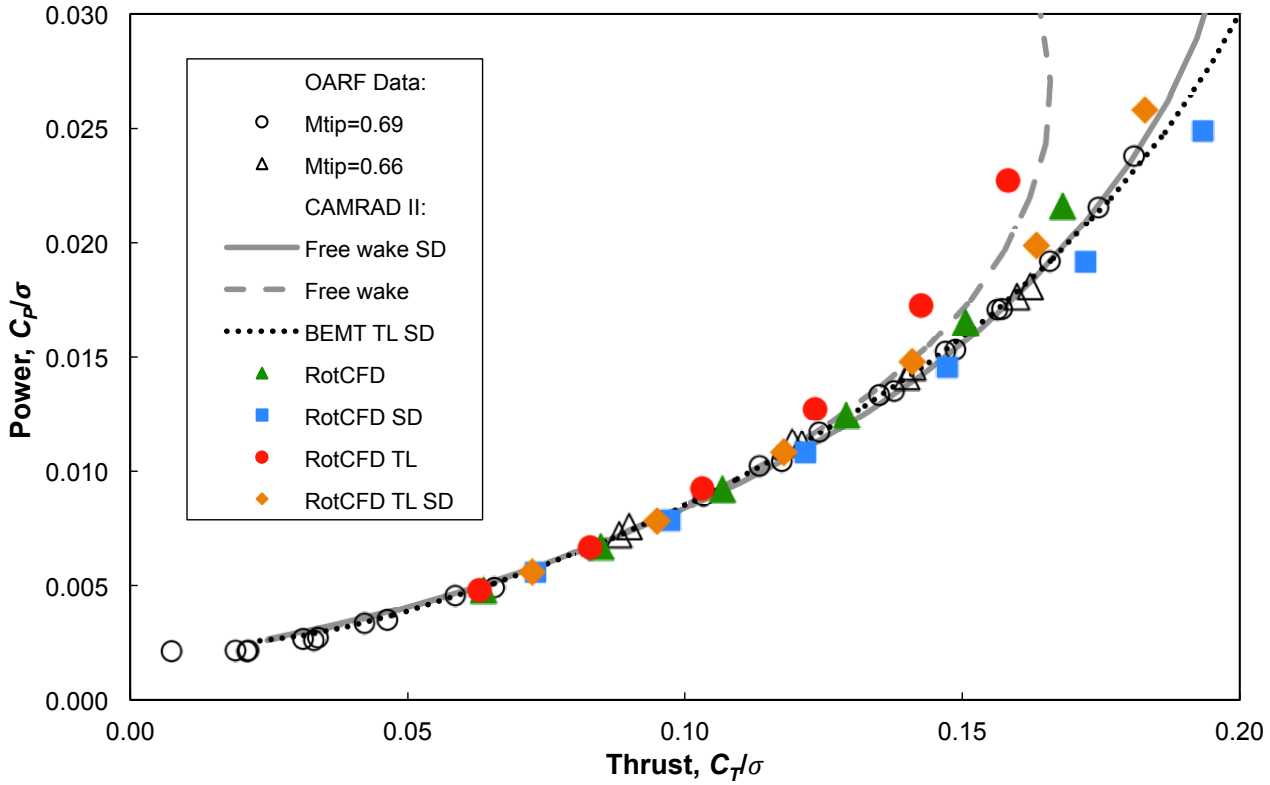

Figure 5. RotCFD results for XV-15 isolated rotor hover power as function of thrust.

Hover performance is also expressed in terms of figure of merit as shown in Figure 6. The RotCFD stall delay model shows very good agreement with the OARF data, especially around peak performance, but tends to diverge a bit towards the higher thrust region after $C_T/\sigma > 0.175$. The tip loss model used by RotCFD is too aggressive, however. RotCFD with stall delay but *no* tip loss ("RotCFD SD") gives results closely similar to blade-element momentum theory with stall delay and Prandtl tip loss ("BEMT TL SD"). Additional analyses with CAMRAD II (not shown) suggest that the Prandtl tip-loss model shifts the predictions only about 1/5 as much as the RotCFD tip-loss model used here. A less aggressive tip-loss model may therefore give RotCFD better correlation with the data. Alternatively, if less likely, the RotCFD stall-delay model may be slightly too aggressive.

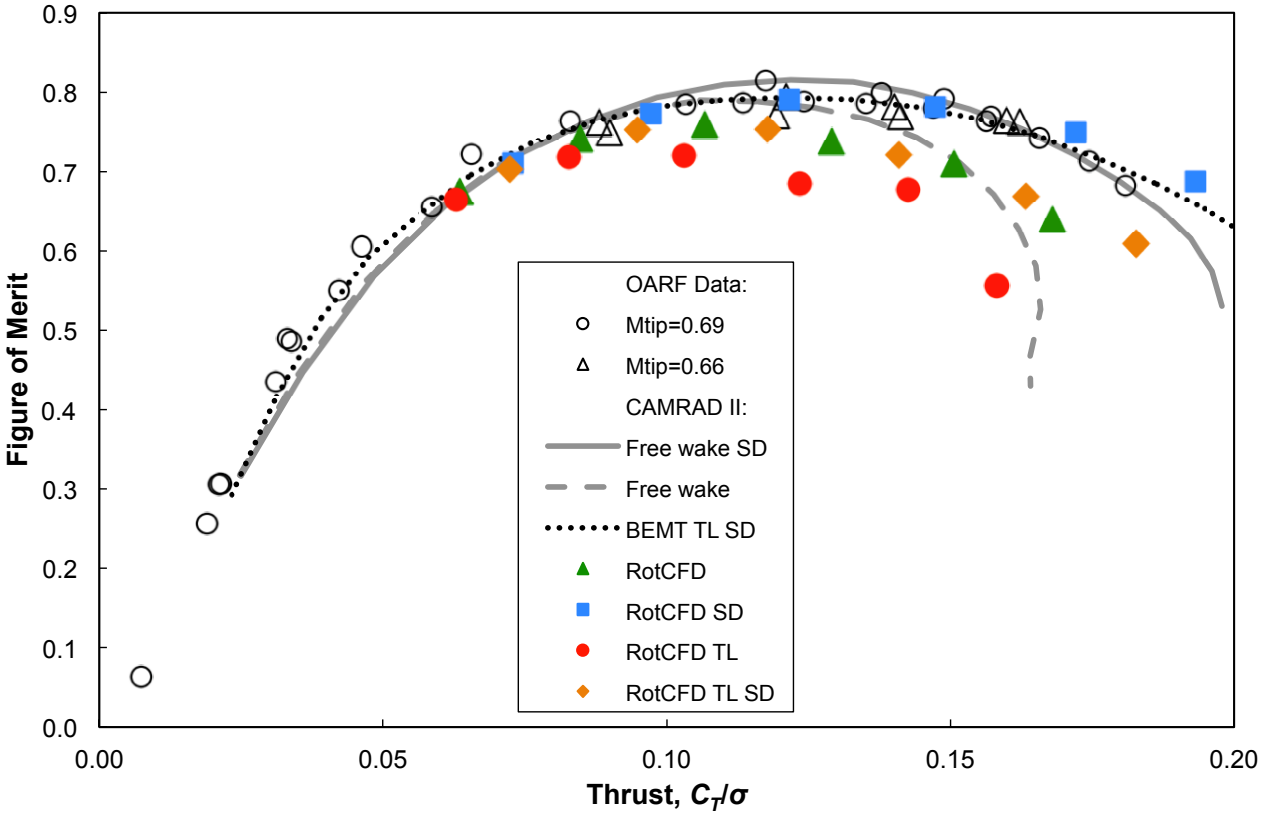

Figure 6. RotCFD results for XV-15 isolated rotor hover figure of Merit as a function of thrust.

2. Tilt Rotor Mode

Figure 7 shows wind-tunnel data for four different pylon angles, all at μ=0.32, M_{tip}=0.65 [16]. The pylon tilt angle α_p varies from 15 deg (near axial flight or airplane mode) to 75 deg (near edgewise flight or helicopter mode). The imposed computational domain within RotCFD are listed in Table 1.

The tilting results were predicted with RotCFD using only tip loss corrections because the stall delay model is optimized for hover and has less effect in tilt rotor mode. The tip loss model yields a more realistic sectional lift distribution along the span by reducing the lift beyond 0.98 r/R. The RotCFD tip loss model, however, is likely not well-matched to the data (recall Figures 5-6). For a tilted pylon at high advance ratio, the influence of tip loss is expected to be minimal because of the relatively low thrust and low induced velocities. A few forward flight conditions were examined with RotCFD with and without tip loss; the effect was negligible (hence not shown in the figures).

RotCFD performance calculations show good correlation with the experimental data. In fact, RotCFD generally matches the data better than CAMRAD II, especially at higher pylon angles. The obvious exception is at α_p=30 deg, but the difference is minor; possible reasons for the mismatch are given following the results for axial flight in the next section.

Improving the CAMRAD II correlation is likely possible by tuning the wake model. The results shown here for CAMRAD II are close to those reported in [17] and no further development of the wake model was attempted. Though the wake is computed directly (not modeled) by RotCFD, the RotCFD results are affected by the computational grid and correlation improvement is expected with a finer grid.

Figure 8 shows the influence of varying the advance ratio under a 75-deg pylon angle. The CAMRAD II predictions diverge substantially from experimental data. The RotCFD predictions show considerably better agreement with the experimental data than CAMRAD II. As with Figure 7, the RotCFD results are very encouraging given the relatively small set-up and execution time required compared to other analyses.

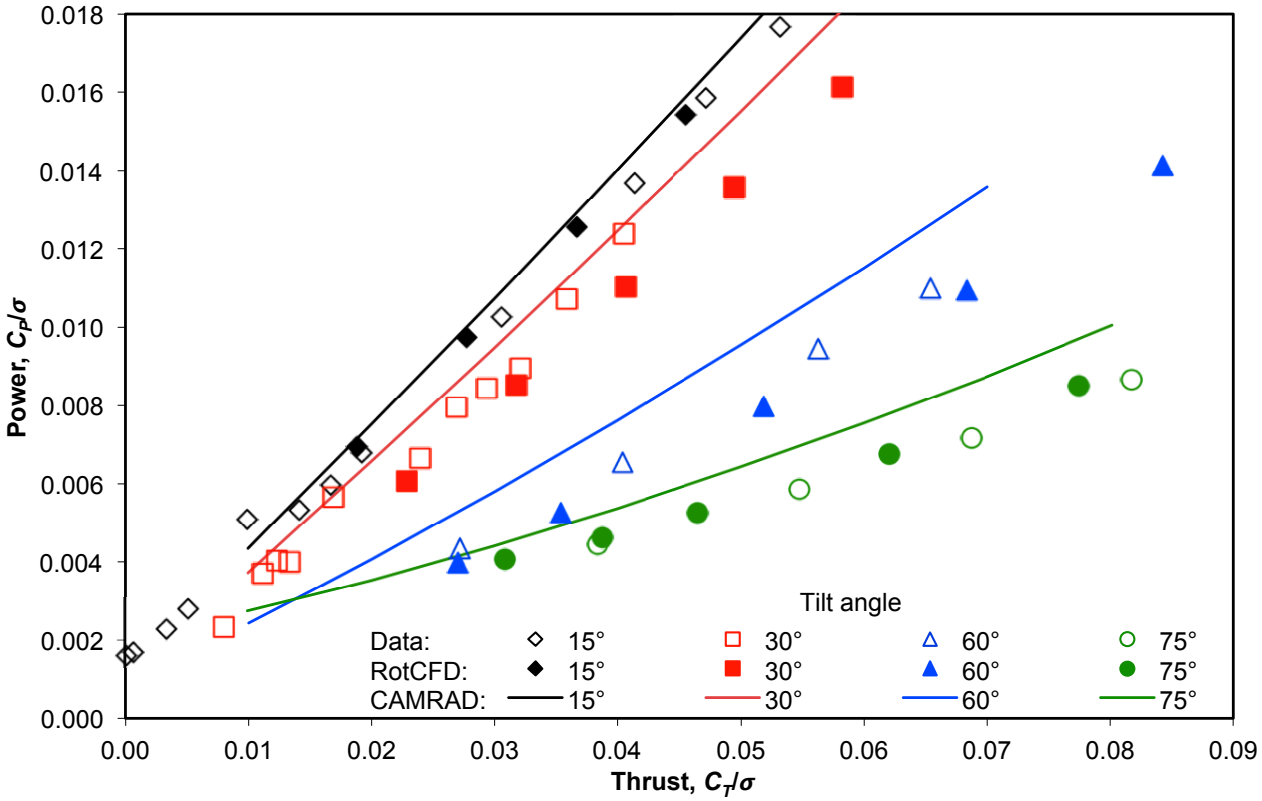

Figure 7. RotCFD results for XV-15 isolated rotor power as a function of thrust for different tilt angles at μ=0.32, M_{tip}=0.65.

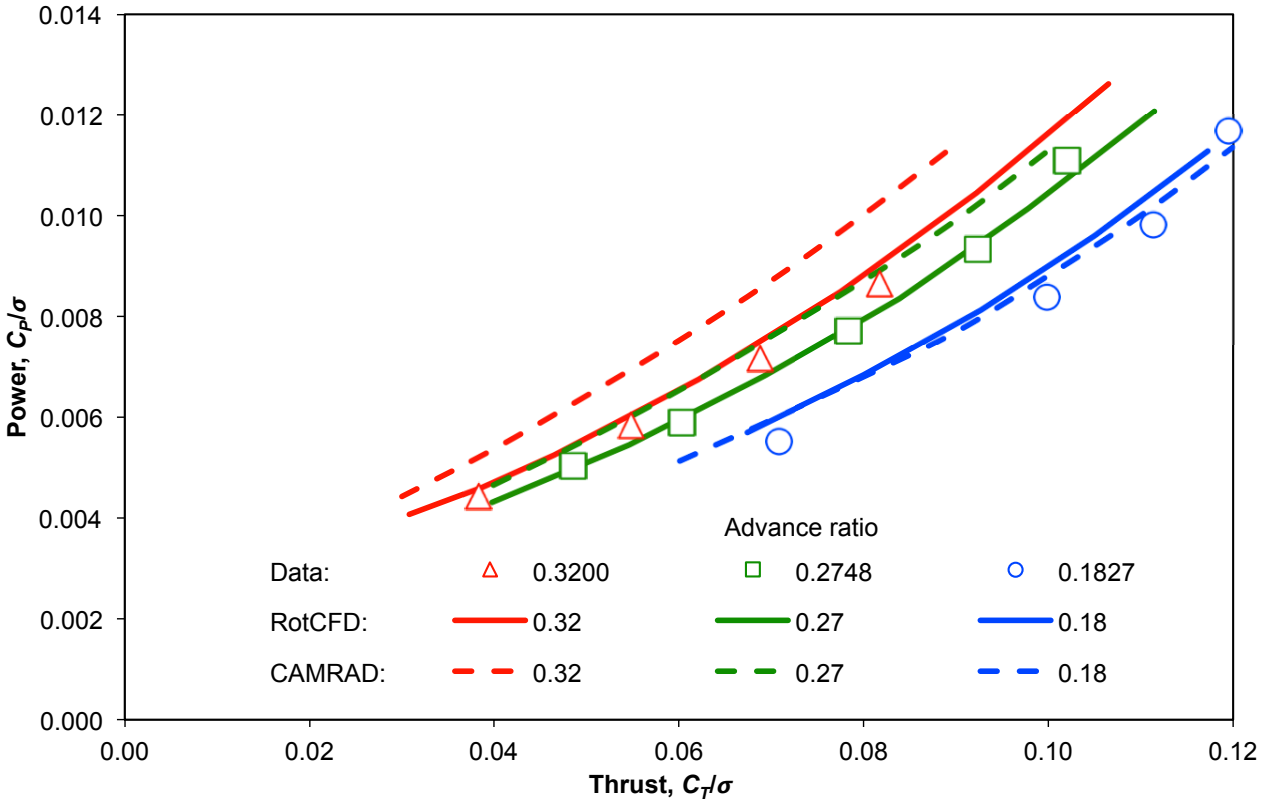

Figure 8. RotCFD results for XV-15 rotor power as function of thrust for different advance ratios at α_p = 75°, M_{tip} = 0.65.

3. Axial Flight

Figure 9 shows the propulsive efficiency in axial flight or airplane mode for two advance ratios. The airplane-mode tip speed is 76% of nominal hover tip speed. Predictions with RotCFD used tip loss corrections only. RotCFD and CAMRAD predictions are given for M_{tip}=0.54 and two values of advance ratio, μ=0.40 and μ=0.70. Johnson [17] shows many more combinations of tip speed and advance ratio, but there were rarely enough data points at any given combination to establish clear trends [16]. The data presented in Figure 9 roughly span the range of measured propulsive efficiency.

Correlation of RotCFD predictions with data at the lower advance ratio, μ=0.40, is reasonable, but predicted propulsive efficiency is low at mid-range thrust. The correlation is nearly identical for RotCFD and CAMRAD II, which implies that the rotor has minimal influence on the external flow field. Such a result is to be expected: at high speed, the thrust coefficient is low, and consequently induced velocity is a small fraction of total velocity. In physical units (not coefficients), the maximum thrust achieved in airplane mode is only 1/5 that in hover. At the higher advance ratio, μ=0.40, the correlation of RotCFD is distinctly worse at mid-range thrust (C_T/σ =0.02-0.04). At this condition, the freestream Mach number is 0.38.

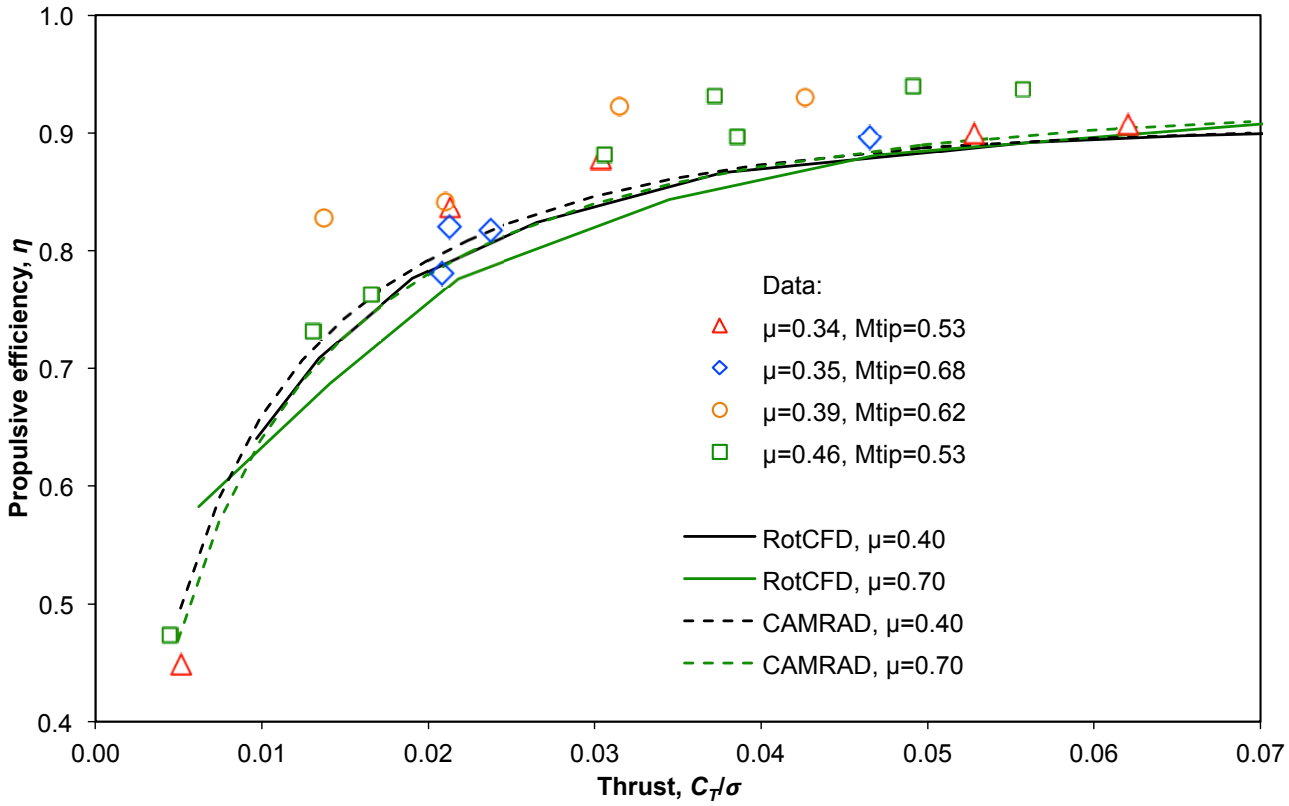

Figure 9. RotCFD results for (rotor) propulsive efficiency as function of thrust.

Some caution should be used when interpreting the results of Figures 7-9. There are several reasons why the predictions may not, or even should not, match the data:

(1) The rotor that was tested was subject to wall effects, especially at high pylon angles. Although RotCFD will eventually be used to estimate the magnitude of such effects on XV-15 performance, all calculations presented in this paper assume an isolated rotor.

(2) The XV-15 rotor has a large spinner with a large drag tare. The wind-tunnel data report [16] shows that spinner drag varies in a nonlinear, nonmonotonic fashion with pylon angle. However, the report also states that "the lift balance data become questionable" during some of the tare measurements, and that final spinner drag tares were estimated from small-scale data. The report does not list spinner drag separately in the data tables, so examining

the tare corrections in detail is not possible. At tilt angles other than zero, spinner drag is not aligned with the rotor shaft and affects both lift and drag as measured by the tunnel scales.

(3) The rotor may have experienced some degree of laminar flow in the protected environment of the wind tunnel. If so, the section drag coefficients would be lower than the coefficients in the airfoil tables and computed power would be lower. Such an effect would explain some, but not all, of the mismatch between predictions and data in Figure 9.

VII. Conclusions and Recommendations

RotCFD was used to predict XV-15 isolated rotor performance for a variety of flight conditions. The effects of stall-delay and tip-loss models were examined in detail for hover, where they are most important. With a stall-delay model, the RotCFD predictions for hover match the data quite well, except at very high values of thrust. However, the tip-loss model appears to be too aggressive.

For tilt rotor mode—pylon angles of 15, 30, 60 and 75 deg—RotCFD usually predicted performance well. For airplane mode, RotCFD often underpredicted propulsive efficiency, but generally no worse so than CAMRAD II.

In general, RotCFD predictions of performance of the XV-15 isolated rotor were adequate to be used as a baseline for investigation of wind-tunnel wall interference effects on performance, which is the intended next step of the research.

As long as a hybrid CFD method such as RotCFD relies on 2D airfoil tables, corrections for stall delay and tip losses are required. RotCFD calculates more detailed information about the flow field than does any blade-element rotor model or the CAMRAD II wake model. Work is underway to use computed blade pressures to construct a more sophisticated tip-loss model.

Planned future work includes refinement of the XV-15 blade geometry within RotCFD, comparison of the discrete-blade solution method to experimental data, and estimating wind tunnel wall effects on the XV-15 performance by modeling the wind tunnel installation in RotCFD.

Acknowledgements

The authors wish to thank Dr. Gloria K. Yamauchi for her patient and insightful advice, without which the research would not have progressed very far.

References

[1] W. P. Jones and B. E. Launder, “The prediction of laminarization with a two-equation model of turbulence,” *Int. J. Heat Mass Transf.*, vol. 15, pp. 301–314, 1972.

[2] B. E. Launder and D. B. Spalding, “The numerical computation of turbulent flows,” *Comput. Methods Appl. Mech. Eng.*, vol. 3, pp. 269–289, 1974.

[3] W. W. Chung, D. Linse, A. Paris, D. Salvano, T. Trept, T. Wood, H. Gao, D. Miller, K. Wright, R. Young, and V. Cheng, “Modeling High-Speed Civil Tiltrotor Transports in the Next Generation Airspace,” NASA CR 215960, pp. 1–414, 2011.

[4] R. G. Rajagopalan, V. Baskaran, A. Hollingsworth, A. Lestari, D. Garrick, E. Sous, and B. Hagerty, “RotCFD - A tool for aerodynamic interference of rotors: Validation and capabilities,” in *American Helicopter Society International - Future Vertical Lift Aircraft Design Conference 2012*, 2012, pp. 311–327.

[5] K. Guntupalli, L. A. Novak, and R.G. Rajagopalan, "RotCFD: An Integrated Design Environment for Rotorcraft," AHS Technical Meeting on Aeromechanics Design for Vertical Lift, San Francisco, CA, January 20-22, 2016.

[6] W. Johnson, "CAMRAD II Comprehensive Analytical Model of Rotorcraft Aerodynamics and Dynamics." Johnson Aeronautics, Palo Alto, 2005.

[7] P. R. Spalart, "Strategies for turbulence modelling and simulations," *Int. J. Heat Fluid Flow*, vol. 21, pp. 252–263, 2000.

[8] Z. Yu and Y. Cao, "Three dimensional turbulence numerical simulation of rotor in forward flight," *Beijing Hangkong Hangtian Daxue Xuebao/Journal Beijing Univ. Aeronaut. Astronaut.*, vol. 32, no. 7, pp. 751–755, 2006.

[9] A. F. Antoniadis, D. Drikakis, B. Zhong, G. Barakos, R. Steijl, M. Biava, L. Vigevano, A. Brocklehurst, O. Boelens, M. Dietz, M. Embacher, and W. Khier, "Assessment of CFD methods against experimental flow measurements for helicopter flows," *Aerosp. Sci. Technol.*, vol. 19, no. 1, pp. 86–100, 2012.

[10] J. G. Leishman, *Helicopter Aerodynamics*, 2nd ed. Maryland: Cambridge University Press, 2006.

[11] J. J. Corrigan and J. J. Schillings, "Empirical Model for Stall Delay Due to Rotation," AHS Aeromechanics Spec. Conf., pp. 8.4 – 1 to 8.4 – 15, 1994.

[12] C. W. Acree, "Modeling Requirements for Analysis and Optimization of JVX Proprotor Performance," in AHS 64th Annual Forum, Montréal, Canada, 2008, pp. 1–21.

[13] W. L. Arrington, M. Kumpel, R. L. Marr, and K. G. McEntire, "XV-15 Tilt Rotor Research Aircraft Flight Test Data Report," NASA CR 177406, vol. 1–5, pp. 1–202, 1985.

[14] M. D. Maisel, D. J. Giulianetti, and D. C. Dugan, "The History of The XV-15 Tilt Rotor Research Aircraft From Concept to Flight," NASA SP 4517, pp. 1–194, 2000.

[15] F. F. Felker, M. D. Betzina, and D. B. Signor, "Performance and Loads Data from a Hover Test of a Full-Scale XV-15 Rotor," NASA TM 86833, pp. 1–94, 1985.

[16] Bell Helicopter Company, "Task II - Wind Tunnel Test Results," NASA CR 114363, 1976.

[17] W. Johnson, "An assessment of the Capability To Calculate Tilting Prop-Rotor Aircraft Performance, Loads, and Stability," NASA TP 2291, pp. 1–21, 1984.

[18] D. C. Dugan, R. G. Erhart, and L. G. Schroers, "The XV-15 Tilt Rotor Research Aircraft," NASA TM 81244, pp. 1–18, 1980.

[19] M. D. Maisel, D. C. Borgman, and D. D. Few, "Tilt Rotor Research Aircraft Familiarization Document," *NASA* TM X-62, 407, pp. 1–105, 1975.